International Journal of Computer Information Systems and Industrial Management Applications.
ISSN 2150-7988 Volume 8 (2016) pp. 115-124

Multi-Agent Segmentation using Region Growing and Contour Detection: Syntetic evaluation in MR Images with 3D CAD Reconstruction

Abdelhafid NACHOUR[1], Latifa OUZIZI[2], Youssef AOURA[3]

ENSAM, Ecole Nationale Superieure d'Arts et Meiters,
Moulay Ismail University
Meknes, Morocco
[1]nachour.abdel@gmail.com, [2]l.ouzizi @ensam-umi.ac.ma, [3]y.aoura @ensam-umi.ac.ma

Abstract: **Computer assisted surgery navigation takes full advantage of progress in engineering disciplines. Developed models increase the accuracy of replacement technique, especially in hip surgery to reduce the risk of component mal-positioning. This paper presents a 3D model reconstruction from contour extracted through a proposed multi-agent segmentation (MAS) approach. We first describe parallel agents' behaviors for extracting the object of interest from MR Images. The proposed algorithm is formulated by combining region growing and contour detection ensuring an overall segmentation. The 3D CAD model is generated using MATLAB code implemented as per the MAS method and gives us good result of reconstruction in most of the cases. The comparison of the proposed method with the traditional approach is made in terms of run times segmentation and edge detection accuracy.**

Keywords: Virtual Surgery; Multi-agent Systems; Segmentation; 3D reconstruction; CAD model; Human Femur.

I. Introduction

A virtual surgery simulation significantly increases the likelihood of obtaining satisfactory results. The simulation refers to replicating a model or a process in a computer [1]. Habitually the starting point is a set of 3D models generated from medical images, usually computed tomography (CT) image or Magnetic Resonance Images (MRI). The establishment of total prostheses assisted by computer is a new technique since the first implantation is dated in 1997 [2]. the principle is to replace damaged joint by resurfacing the bone end of the thigh and hip bone, capping them with metal, to ensure support, flexibility and motion, without pain. The 3D models are used as reference in the virtual surgery to determine the patient-specific implant geometry [3]. These models have recently been applied to various applications [4]-[7]. The required models decrease the preoperative workup time and increase the accuracy of model preparation and subsequent surgery. This 3D models are reconstructed from MR Image that produce high image quality of human bone. 3D Image-based reconstruction techniques can be divised in three major parts, such as depth-map-based approaches, volume-based approaches, and surface-based approaches [8]. Following image acquisition, the preoperative traitements in the 3D reconstruction consist of: (i) Segmenting images into objects, (ii) assessment of objects of interest, (iii) set of cross-sectional objects of interest contours.

Image segmentation refers to the technique that partitions a digital image into set of segments typically used to identify regions of interest (Regions of Interest, ROI) or other relevant information in digital images [9] based on criteria such as similarity and homogeneity. According to Cocquerez, [10], the choice of a technique is linked to the nature of the image and the treatments after this segmentation. The existing image segmentation algorithms can be classified into four categories [11]: (1) Local filtering approaches, (2) Snake and Balloon methods, (3) Region growing and merging techniques, and (4) Global optimization approaches based on energy functions or Bayesian and MDL (Minimum Description Length) criteria. Region growing method has been widely used for image segmentation [12], and in particular medical image applications. It is a region-based segmentation in which pixels are segmented by grouping similar neighboring pixels of seed points [13]. For example, if a similarity measure of the two adjacent pixels is greater than a threshold, these pixels are similar and thus are grouped together. The grouping of neighboring pixels continues until no similar pixels remain. However, two major problems plaguing the traditional region growing algorithms: first the difficulties to select the appropriate initial seed automatically, second, the noises and regions with holes form [14]. For the first problem, automatic

segmentation algorithm by integrating color-edge extraction and seeded region growing is done in [15]. The authors use an Edge detection algorithm conducted on the image to obtain the major geometric structures as an intermediate to select the initial seeds. Approximate center point of the lesion region is taken as the initial seed in the automatic seed point selection algorithm proposed in [16]. For the second problem, the usual practice is to remove the noise by Gaussian filtering [16], [17] or median filtering [18], [19] applied before segmentation. However, this tool often causes two problems: edge blur [20] and over segmentation [21]. Over segmentation is the process by which the objects of interest are themselves segmented or fractured into regions. Based on the existing algorithms in optimization theory, there are two main approaches to attacking the problem [22]: using random operators and employing multi-individual (agents) based algorithms.

The field of multi-agent systems (MAS) arose during the late 80s when several researchers started to work with mobile robots performing coordinated task [23]. So far, it is currently a very active field of research for many types of applications [24]-[27] and disciplines where the medical interest has increased considerably. The MASs are distributed applications consisting of relatively independent modules called agents, which sometimes employ artificial intelligence techniques to accomplish complex operations [28],[29]. The Multi-agent are used as a useful approach in medical practice, especially, in real-time applications. Various applications of MASs have been proposed in image segmentation where a distributed agent makes possible to apply more advanced algorithms and to perform demanding tasks quickly. Liu et al. [30] and Rodin et al. [31] present a parallel image processing system based on simple reactive agents. Agents act according to a perception–action model without problem solving or deliberation. Bovenkamp [32] elaborate a high-level knowledge-based control over low-level image segmentation algorithms. The agents dynamically adapt segmentation algorithms based on knowledge about global constraints, contextual knowledge, local image information and personal beliefs. Settache et al. [33] use multi-agent system to share the result of a quad three algorithm used to identify regions primitive, and a Shen filter used to determine edges in the MRI brain part's detection. Bellet et al. [34] present incremental processes of region growing and edge detection where the cooperation between two types of agent is dynamic and allows to transmit informations when it becomes necessary for a taking of decisions. This cooperative approach increases the segmentation's quality by confronting the information provided from different algorithms. Yanai et al. [35] use a MAS to extract primitives information like lines, edges or regions using different types of algorithms. Each agent is located on the image and builds a set of coherent primitives. Then, the agents interact to negotiate their local primitives.

In this paper, we develope a multi agent segmentation approach for 3D CAD model reconstruction of human femur from MR Images. We first present a parallel agents' behaviors for extracting the object of interest by combining region growing and contour detection ensuring an overall segmentation (Fig1). This is similar to the convergence of individuals in multi-agent optimization algorithms [36]-[38], in which each agent starts from different initial seed but they are all supposed to converge to the best possible solution. We use two reactive agent equipped with ability to define pixels with the same primitive which discern regions and edges: ''Region'' agents to solve the particular difficulty of region growing algorithm and ''Edge'' agents for overall segmentation. Each agent is responsible for the detection of exactly one type of image object and can be communicate with each agent doing its image interpretation in parallel with others agents. The results of the segmentation step are used for the proposed 3D reconstruction of the bony elements. The 3D CAD model is generated using MATLAB code implemented as per the MAS method and gives us good result of reconstruction in most of cases.

The paper is organized as follow: in the next section, the proposed method for 3D image recostruction is presented. Section III presents the results of a 3D CAD model of human femur. Finally, section IV is devoted for conclusion.

II. Proposed 3D reconstruction

The approch adopted in this paper has three steps. At first, the MR Images are exported from DICOM format(Digital Imaging in Medicine and Communications) to JPEG type with dimensions of 200×550 pixels. The second step focuses on segmentation technique using multi-agent system to extract the edge of the femur and the process of 3D CAD model reconstruction is developed in third step.

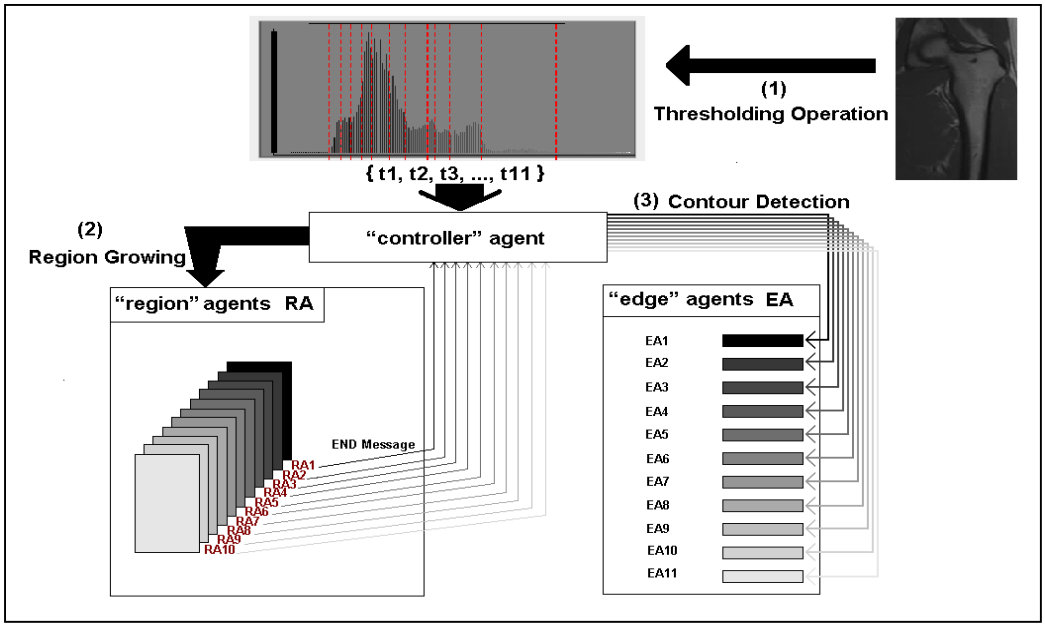

Figure 1. Operational MAS steps. (1) Thresholding operation produces 11 thresholds value for MR Image, (2) Controlller agent initiates the region growing algorithm with 10 agents, and (3) Edge detection after each end message where the last agent represent the image borders.

A. MR Image multi-agent segmentation

One of the major problems encountered in medical image segmentation is to separate the regions and edges corresponding to object of interest, from the regions that correspond to the background. The proposed MAS is constituted by the agents and their environment which contains the images. Each pixel of image is characterized by a gray level and boolean value which defines if the pixel has already been explored by an agent. We use three types of agents initialized automatically:

- Agent named "controller" contains all information required to initialize and operate others agents.
- Agents named "region" responsible to segment homogeneous regions.
- Agents named "edge", represent region's boundaries.

Each agent is further responsible for one processing task and cooperates with other agents to come to a consistent overall image segmentation. JADE (Java Agent Development Framework) created by TILAB laboratory and described by Bellifemine et al. [39] is used to build the system. In the following sub-sections, we define each agent as well as their interactions.

1) controller agent:

In the first operational step, "controller" agent is responsible for initializing each "region" agent. For instance, if there are n class region in the image, n "region" agents should be created. In this step, unique "region" agent is defined for each class. In order to obtain a completely automatic segmentation, seed pixels that initiate region growing algorithm, are determined the first step using thresholding operation in histogram processing [40].

After each end message from "region" agents, "controller" agent activates the "edge" agent to create the boundaries of the last region.

2) Region agent:

The "region" agent receives a seed pixel and moves to its neighbors and iteratively merges pixels into sets, according to homogeneity criteria (Fig.2).

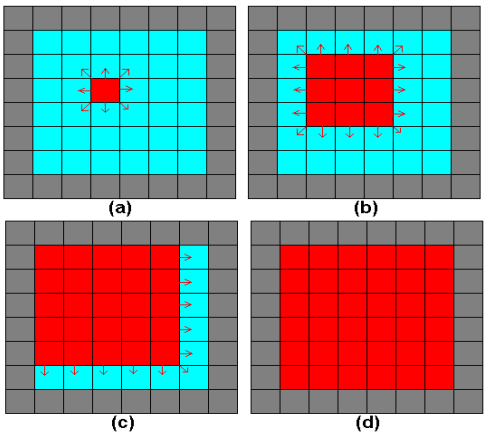

Figure 2. Region growing algorithm: (a) represent seed pixel in red (b) (c) region growing process by adding homogenious neighbors pixel and (d) represent segmented region.

Homogeneity is defined according to the local statistics of the window formed for each image pixel [41]. To determine whether the pixel neighbors should be added to the region, homogeneity is calculated using two parameters: standard deviation and discontinuities (gradient norm). The standard deviation describes the brightnesse within a region with n pixels (n=9 in our case), and the discontinuity indicates an abrupt change in gray level of pixel neighbors. If a similarity measure $|H(P)-H(Pn)|$ of the two adjacent pixels P and Pn is less than a pre-defined threshold ε, these pixels are similar and thus are grouped together. The grouping of neighboring pixels continues until no similar pixels remain.

We consider I_{ij} the intensity of the pixel P_{ij} at the position (i,j) in image SMN where (M, N) is the image dimensions, $0<i<M$ and $0<j<N$. The local mean of gray level m_{ij} of the

pixel P_{ij} is calculated over a window of size d×d centred at P_{ij} using the following equation (1):

$$m_{ij} = \sum_{p=i-\frac{d-1}{2}}^{p=i+\frac{d-1}{2}} \sum_{q=j-\frac{d-1}{2}}^{q=j+\frac{d-1}{2}} (I_{pq}) \quad (1)$$

The standard deviation (variance) e_{ij} of the pixel P_{ij} is calculated using equation (2):

$$e_{ij} = \sqrt{\frac{1}{d^2} \sum_{p=i-\frac{d-1}{2}}^{p=i+\frac{d-1}{2}} \sum_{q=j-\frac{d-1}{2}}^{q=j+\frac{d-1}{2}} (I_{pq} - m_{ij})^2} \quad (2)$$

The discontinuity v_{ij} is calculated using Sobel operator:

$$v_{ij} = \sqrt{G_x^2 + G_y^2} \quad (3)$$

Where $G_x^2$and $G_y^2$are the components of gradient g_{ij} in x and y direction.

Homogeneity $H_{ij}$of pixel $P_{ij}$is calculated using this equation:

$$H_{ij} = 1 - (V_{ij} \times E_{ij}) \quad (4)$$

Where E_{ij} and V_{ij} are respectively the normalized standard deviation and the normalized measure of discontinuity.

The following algorithm shows the incrementing procedure of the region:

Algorithm 1: Region Growing

- Step 1: For each pixel "P" in the image "[S]"

If the pixel "P" is not associated with an agent region, then compute H(P).

- Step 2: Create a new region "[R]" and Add "P" in the region "[R]"
- Step 3: Create the list "[N]" of neighboring pixels of "P".
- Step 4: For each pixel "Pn" in the "[N]"

If |H(P)-H(Pn)|< ε

Then the window of pixel Pn is homogeneous. Add pixel "Pn" in the region "[R]" and Add neighboring pixels of "Pn" in "[N]"

Otherwise, the window of pixel Pn is not homogeneous.

As stated, the use of agent overcome the problem of traditional region growing Algorithm. When the fronts converge to an edge, there is no guarantee that this is a real edge. To increase the probability to find a real edge, the value of ε should be close to 0.

3) Edge agent:

After applying the region growing algorithm, "edge" agents is initiated to determine the region boundaries using the following algorithm:

Algorithm 2: Edge Detection

- Step 1: For each pixel "P" in the "[R]":

Create list "[N]" of neighbor's pixels of "P"

- Step 2: For each pixel "P_n" in the list "[N]":

if "P_n" is not in "[R]" then add pixel "P_n" in the edge "[C]"

During this final step, all pixels located at the boundaries of the obtained regions are identified by "edge" agents (Fig.3). Extracted edge provides a concise, closed and accurate representation of regions boundaries in the image.

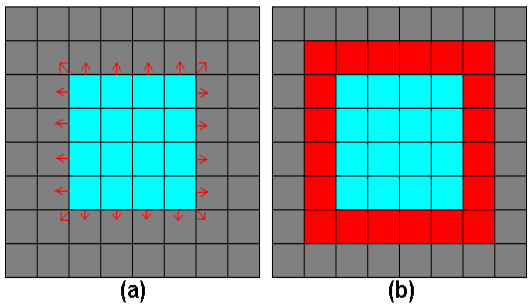

Figure 3. Edge detection result of "edge" agent: red color in (b) represent the obtained edge for the cyan region in (a).

4) Agent communication:

An agent can communicate with others agents to establish relations, and exchange interests, capabilities, and image interpretations. In the present system, the communication agent language used is the FIPA ACL [42] that provides the types of required message. The communication between agents is summarized in the following Fig.4:

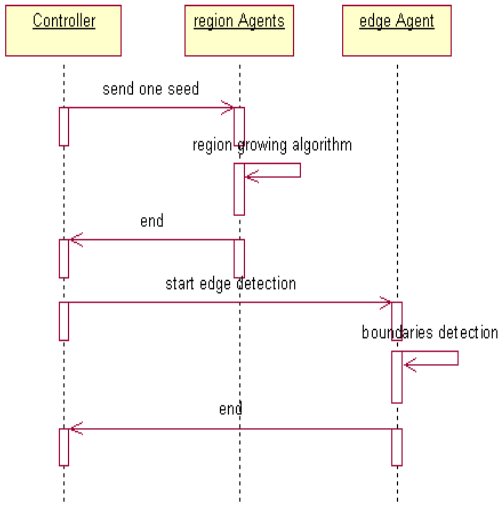

Figure 4. The communication process between agents.

B. 3D CAD reconstruction prosses

In this work, we use MATLAB package containing algebraic iterative methods for 3D reconstruction. The whole set of 16 images is concatenated one on top of the other into a matrix of size 200×550×16. The 3D matrix is then converted into a surface or set of surfaces using isosurface techniques. The surface is defined by the z-coordinates of points above a rectangular grid in the x and y plans. The surface is formed by joining adjacent points with straight lines.

A surface function S(d) is defined as the summation of the square distance between two corresponding points $U_{i,j}$ and $U_{i+1,j}$ in the edges C_i and C_{i+1}respectively. For the two sets of the uniformly distributed points, $\{U_{i,j}\}_{i=0,\ldots,m}$ and $\{U_{i+1,j}\}_{j=0,\ldots,n}$, the penalty function S(d) is defined as follows:

$$S(d) = \sum_{l=0}^{n+m} \left\| U_{i,l} - U_{i+1,l+d(\mathrm{mod}(n+m))} \right\|^2 \quad (5)$$

The basic code incorporated in this program can be found as an example for 3D reconstruction in the Help option of MATLAB 6 [43].

III. Results and discussion

We have developed and tested the application which is written in JAVA and use MATLAB package. We present some results of the MAS human femur segmentation compared to the traditional approach. Experiments were done on a core duo (2.2 GHz, 2 GB), using the Windows XP. We have used a single square window 3×3 which is kept constant through all the experiments. The major technical challenge is to extract some typical 3D geometry parameters with respect to the patient's 3D bone anatomy.

A user interface is presented in Fig.5 and contains four buttons which initiate separate functions of the program and a panel to show results.

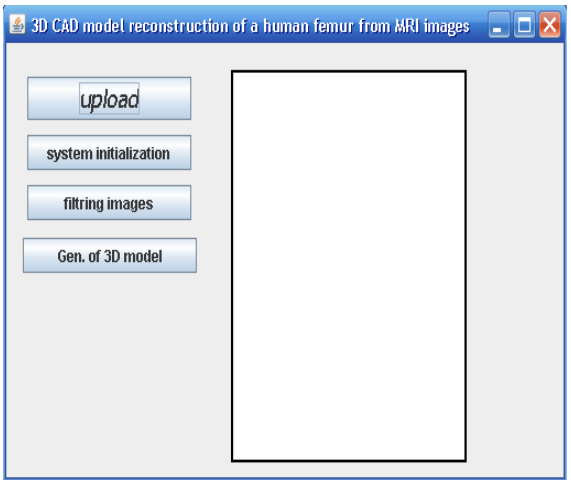

Figure 5. The user interface of our application.

The first button allows uploading images, the whole set of images will be displayed as an MR Images film. Then the images will be segmented by clicking on the second button. If the images demand filtering, this process can be initiated by the click on the third button or this step can be skipped. The filtration function is programmed for smoothing (low pass) filters that reduce noise.

The segmentation approach described in Section II.A is applied on MR Images in sagittal view. The set of 16 images are used in transversal plan (Fig.6). The whole set of images will be displayed as a MRI film. We present the results about one patient and similar behaviors are observed with other patients MR Images.

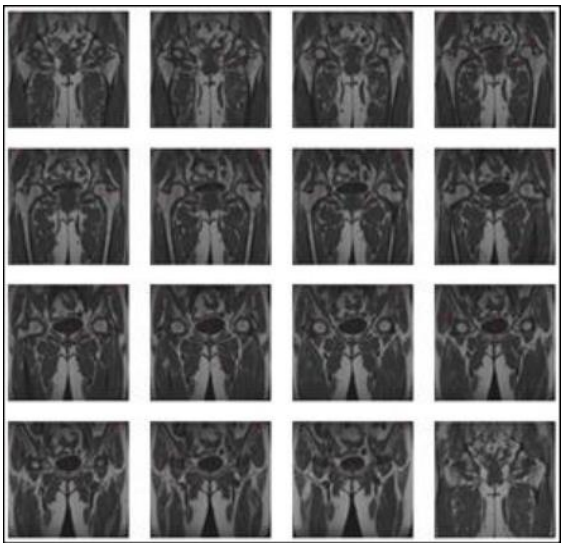

Figure 6. MR Images of human femur in sagittal view.

The filtered images are segmented using ''region'' and ''edge'' agents. Fig.7 chows a result of edges end regions detection in a single image where 158 ''region'' agents are created for 158 thresholds obtained using histogram analysis with $\varepsilon = 0{,}3$.

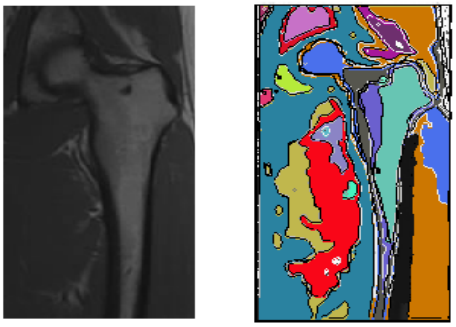

Figure 7. Edges end regions detection in a single image. (a) origin image and (b) segmented image where the colors are chosen arbitrary for regions and black for edges.

These regions are enveloped using 158 ''edge'' agents. The number of agent is depended on ε which, with a close value to 0, increases the number of agents and consequently the chances of finding a global segmentation. In order to analyze the segmentation accuracy, which depends on the number of initialized agents, we take experiments for human femur series segmentation using different value of ε.

Table 1 shows for varied values of ε, the number of agent created for a single image in Fig7. Fig.8 shows the result of all 16 MR Images used in this work and used for the comparison step.

Values of ε.	Multi-agent approach		Classical approach	
	Number of ‘‘region’’ agents	Run times (s)	Number of classes	Run times (s)
2	3	11,05	3	25,6
1,5	8	11,05	8	28,05
0,9	55	10,26	55	35,11
0,7	104	7,33	104	49,72
0,5	125	6,05	125	50,88
0,3	158	6,02	158	51,29

Table1. comparison of the proposed method with the traditional aproach in run time process with varied values of ε.

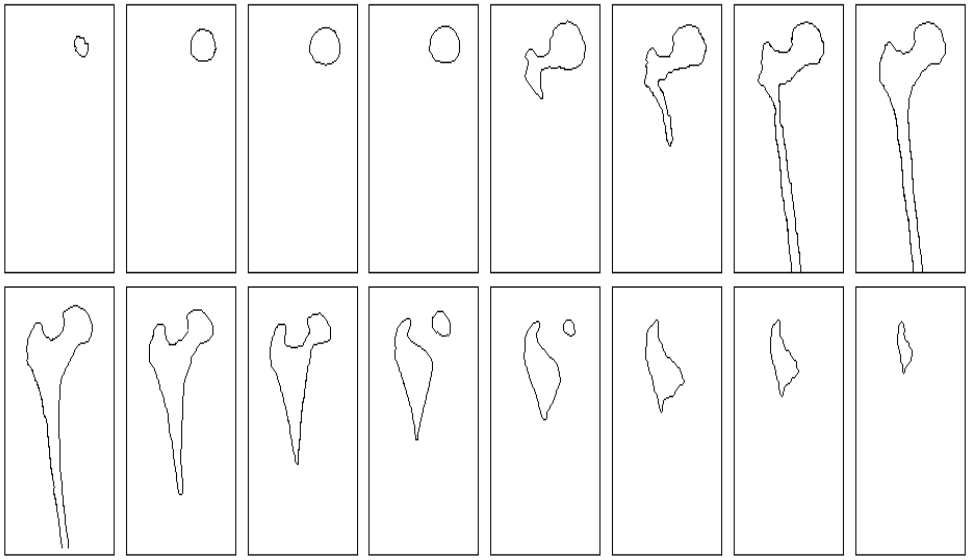

Figure 8. Result of detection for 16 used MR Images

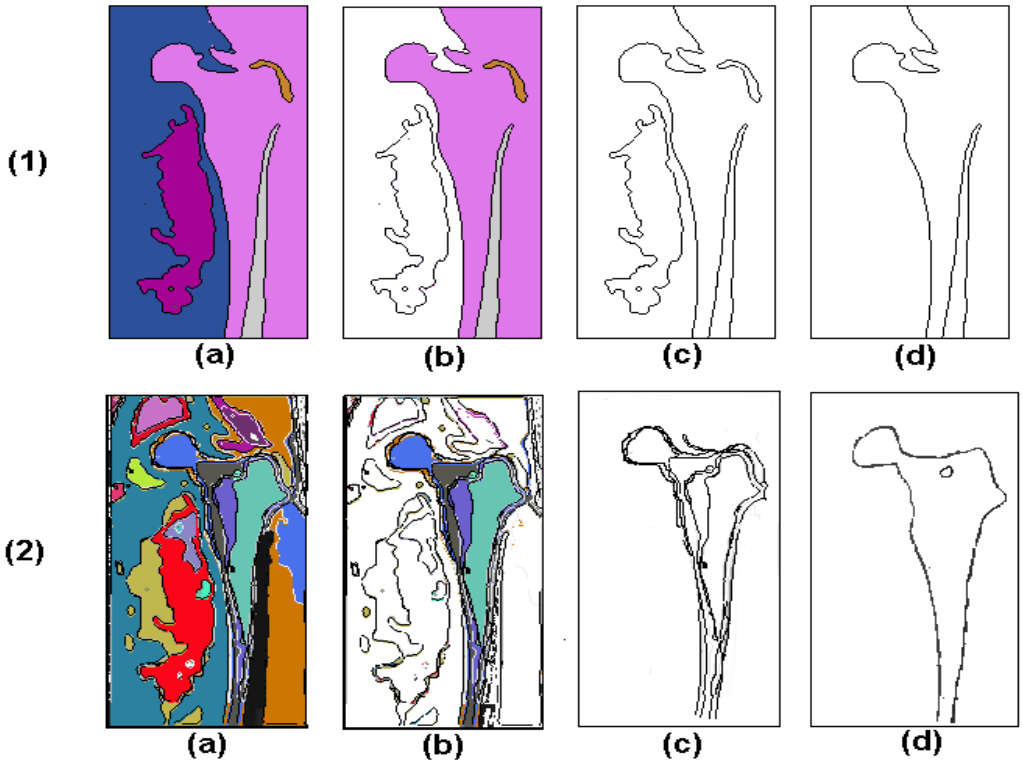

Figure 9. Exemple of selected edge agent in a single layer for two values of ε where in (1) ε=2 and in (2) ε=0,3. (a) object of interest selection, (b) to (c) choosing the edge of interest.

Depending on the selection of ε, the traditional approach is capable of finding the classes within the image. Hence, the smaller value of ε, the longer the convergence time and the higher the probability to find more details that exist in the image. Moreover, even by using a multi-agent system, there are some cases where the procedure cannot segment accurately (Fig.9 (1)). The probability of finding the best segmentation can be improved by increasing the number of agents (Fig.9 (2)). As can be observed in Table.1, the run time process decrease when the smaller value of ε is chosen due to parallel treatment of agents.

To accurately evaluate the performance of the method adopted in this work, the results performance are quantified in terms of good detection (SNR) and good localization (GL) [44]. In the discrete case, the SNR can be approximated by:

$$SNR = (\frac{N_r}{N_e})(\frac{N_{ne}}{N_f + 0,1}) \qquad (6)$$

Where N_r is the number of pixels detected correctly as an edge pixels and N_f denotes the number of pixels detected incorrectly as an edge pixels, respectively, N_e and N_{ne} are the number of real edge pixels and non-edge pixels respectively. The GL [45], [46] is defined as:

$$GL = (\frac{1}{\max(N, N_d)}) \sum_{i=1}^{N} \frac{1}{(1 + d_i^2 e)} \qquad (7)$$

Where N and $N_d = N_r + N_f$ are real and detected edge pixels respectively, d_i is the Euclidean distance between the ith detected edge pixel and the nearest real contour pixel, and e is a constant typically set to 1/9 [44]. GL ranges between 0 and 1.

Table.2 shows the performance criterion using these metric with a single threshold for the whole set of 16 MR Images compared with others segmented manually. The results of SNR and GL are superior to the others in the classical method and the total time segmentation was approximately 2X to 8X faster.

N ° image	Multi-agent approach			Classical approach		
	SNR	*GL*	Time (s)	*SNR*	*GL*	Time (s)
1	83	0.988	6	42	0.825	51
2	104	0.985	6	40	0.828	51
3	147	0.988	6	55	0.835	51
4	169	0.98	6	104	0.849	51
5	178	0.985	6	125	0.85	51
6	158	0.988	6	129	0.851	51
7	158	0.975	6	117	0.834	51
8	163	0.975	6	112	0.843	51
9	158	0.97	6	137	0.832	51
10	147	0.978	6	125	0.83	51
11	130	0.975	6	129	0.812	51
12	158	0.981	6	116	0.832	51
13	152	0.985	6	120	0.812	51
14	104	0.979	6	104	0.843	51
15	84	0.985	6	35	0.858	51
16	93	0.98	6	41	0.834	51

Table2. comparaison of the proposed method with the traditional aproach in terms of good detection SNR and good localisation GL.

The fourth button initiates the 3D reconstruction using predefined functions in MATLAB software. The wall images are concatenated one above the other, forming a 3D matrix (Fig.10).

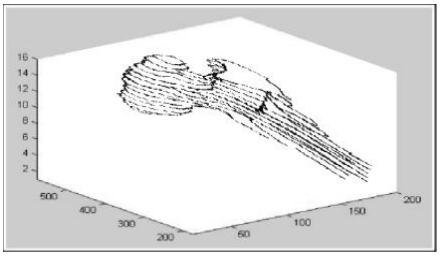

Figure 10. Viewing 3D slices.

After having the 3D model, an STL file format is generated (Fig.11). It can be used by all CAD software and gives possibility to identify the cylinder axis which represents the bone and the sphere center representing femoral head. This tool allows the surgeon to make quickly the necessary decisions regarding the selection and positioning of the implants in 3D and reduce the risk of a mal-aligned component. The Accuracy of the final implant is important to surgeons, and the capabilities of the proposed system to choose object of interest affect the outcome of implant accuracy.

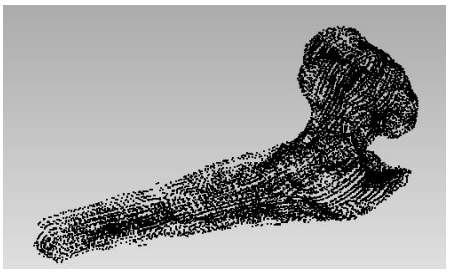

Figure 11. STL file format of human fumer.

Table 3 shows that the model computed from results of segmentation in Fig.9, is in good agreement compared with our works in [47] that use the Active Contour Models [48]. We compare the computed model volume with the standard model volume of human femur generated from manual segmentation. The proposed approach has a lower error calculated according to [49].

	Maximum Errors	
tests	Our approach	Model generated in [47]
1	0.694	1.573
2	0.713	1.573
3	0.708	1.573
4	0.691	1.573
5	0.71	1.573
6	0.698	1.573
7	0.712	1.573
8	0.705	1.573
9	0.696	1.573
10	0.692	1.573

Table3. Maximum Errors compared with the standard model of human femur.

These values depend on the selected agents contours, and the best value is 0.691. The reasons for the superior results given by this approach are: First, it follows that each agent region is always surrounded by edge agent. Secondly, increasing the number of agents decreas the run time and gives the best segmentation.

I. CONCLUSION

Computer assisted placement technique is an accurate and reproducible technique for hip surgery. The purpose of this study is to quantify the accuracy of automated segmentation methods using a multi-agent system.

As a distributed system, the MAS contain a set of agents working together and can generate an overall segmentation. This system is applied to human femur MR Images which are segmented. The parallel agents' behaviors is used for extracting the object of interest by combining region growing and contour detection ensuring an overall segmentation. In addition, the proposed approach is very amenable to manual selection of the object of interest by choosing interest agents. The results of the segmentation step are used for the proposed 3D reconstruction.

The reconstructed 3D CAD model is used to extract parameters like anatomical femoral axis, femoral head center and radius, femoral neck isthmus, femoral neck shaft angle…, which influence the accuracy of the resulting patient-specific implant geometry. This parameters allow the surgeon to make quickly the necessary decisions regarding the selection of the implants in 3D and reduce the risk of misaligned component.

Thanks to our proposed method, we obtained more information in the combined region and edge detection while preserving the edges to the same degree as the regions using the multi agent system. Although we obtained good results, there remain situations in practice, where some user-interaction is desirabl. To integrate user-interaction effectively, we are working on the implementation of a user-agent to allow the user to act as an additional agent in the system. This agent will be used to determine the prior knowledge function of the objects present in the image to be interpreted, depending on their location in the image, and depending on the treatment they have to achieve to reach their goals.

Based on our experiments in MR Image, situated and cooperative agents appear as an interesting framework to implement treatment required for tissue interpretation. As shown with the case of human femur contour, structure identification should be performed to improve tissue identification. For this purpose, anatomical knowledge should be introduced using, possibilistic logic [3]. This can be elegantly performed into our framework via the insertion of new maps, new models and new agents to manage them

References

[1] J. Juan Jiménez, Félix Paulano, Rubén Pulido, J. Roberto Jiménez. ''Computer assisted preoperative planning of bone fracture reduction: simulation techniques and new trends'', *Medical Image Analysis*, 2016.

[2] D. Saragaglia, F. Picard. ''Computer assisted implantation of total knee endoprosthesis with no pre-operative imaging: the kinematic model''. *In: Stiehl JB, Konermann WH, Haaker RG, éds. Navigation and robotics in total joint and spine surgery. Berlin, Heidelberg: Springer-Verlag*, pp. 226-33, 2004.

[3] A. Nachour, L. Ouzizi, Y. Aoura. ''Multi-Agent 3D Reconstruction of Human Femur from MR Images''. In *Proceedings of the IEEE International Conference on Intelligent Systems Design and Applications*, pp. 88-92, 2015.

[4] B. Guenoun, F. El Hajj, D. Biau, P. Anract, J-P. Courpied. ''Reliability of a New Method for Evaluating Femoral Stem Positioning After Total Hip Arthroplasty Based on Stereoradiographic 3D Reconstruction'', *The Journal of Arthroplasty*, 30, pp. 141-144, 2015.

[5] M. J. Schroeder, C. Krishnan, Y. Dhaher, The influence of task complexity on knee joint kinetics following ACL reconstruction. Clinical Biomechanics. 30, pp:852–859, 2015.

[6] P. Zysset, D. Pahr, K. Engelke, H.K.Genant, M. R. McClung , D. L. Kendler, C. Recknor, M. Kinzl, J. Schwiedrzik, OlegMuseyko, A.Wang, C. Libanati. ''Comparison of proximal femur and vertebral body strength improvements in the FREEDOM trial using an alternative finite element methodology'', *Bone*, 81 pp. 122-130, 2015.

[7] D. Dimitriou, T.Y. Tsai, B. Yue, H.E. Rubash, Y.-M. Kwon, G. Li. ''Side-to-side variation in normal femoral morphology: 3D CT analysis of 122 femurs'', *Orthopaedics & Traumatology: Surgery & Research*, 102, pp. 91-97, 2016

[8] Gunay M. *Three-dimensional bone geometry reconstruction from X-ray images using hierarchical free-form deformation and non-linear optimization*, Pittsburgh: Carnegie Mellon University, 2003.

[9] S.A. Hojjatoleslami, J. Kittler. ''Region growing: a new approach'', *IEEE Trans. Image Process*, 7 (7), pp. 1079-1084, 1998.

[10] J. P. Cocquerez et S. philipp. *Analysis of images: filtering and segmentation*, physics education, Ed. Masson, 1995.

[11] X. Zhang, X. Li, Y. Feng. ''A medical image segmentation algorithm based on bi-directional region growing'', *Optik* 126, pp. 2398-2404, 2015.

[12] SW Zucker. ''Region growing: childhood and adolescence''. *Comput Gr Image Process*, 5(3), pp.382-99, 1976.

[13] C. H. Wei, S. Y. Chen, X. Liu. ''Mammogram retrieval on similar mass lesions'', *Computer methods and programs in biomedicine*, 106(3), pp. 234-248, 2012.

[14] R. Rouhi, M. Jafari,S. Kasaei, P. Keshavarzian. ''Benign and malignant breast tumors classification based on region growing and CNN'', *Expert Systems with Applications*, 42, pp. 990–1002, 2015.

[15] J. Fan, D.K.Y. Yau, A.K. Elmagarmid, W.G. Aref. ''Automatic image segmentation by integrating color-edge extraction and seeded region growing'', *IEEE Trans. Image Process*, 10 (10), pp. 1454-1466, 2001.

[16] J. Shan, H.D. Cheng, Y. Wang. ''A novel automatic seed point selection algorithm for breast ultrasound images'', in *The 19th International Conference on Pattern Recognition(ICPR)*, pp. 1-4, 2008.

[17] Z. Pan, J. Lu. ''A Bayes-based region-growing algorithm for medical image segmentation'', *Comput. Sci. Eng*. 9 (4), pp.32-38, 2007.

[18] D. A. Forsyth, J. Ponce. *Computer vision: A modern approach*. Upper Saddle River, NY: Prentice Hall, 2003.

[19] A. K. Mohanty, M. R. Senapati, S. K. Lenka. ''A novel image mining technique for classification of mammograms using hybrid feature selection'', *Neural Computing and Applications*, 22 (6), pp. 1151-1161, 2013.

[20] Z. Lin, J. Jin, H. Talbot. ''Unseeded region growing for 3D image segmentation'', in: *Workshop on Visualisation*, 2, pp. 31-37, 2000.

[21] P. Asmussen, O. Conrad, A. Günther, M. Kirsch, U. Riller. ''Semi-automatic segmentation of petrographic thin section images using a "seeded-region growing algorithm" with an application to characterize wheathered subarkose sandstone'', *Computers & Geosciences* 83 pp. 89-99, 2015.

[22] A. Kasaiezadeh, A. Khajepour. ''Multi-agent stochastic level set method in image segmentation'', *Computer Vision and Image Understanding*, 117, pp. 1147-1162, 2013.

[23] T. Arai, H. Ogata, T. Suzuki. ''Collision avoidance among multiple robots using virtual impedance'', In *Proceedings of the IEEE/RSJ international conference on intelligent robots and systems*, pp. 479-485, 1989.

[24] Z. Li, J. Liu. ''A multi-agent genetic algorithm for community detection in complex networks'', *Physica A: Statistical Mechanics and its Applications*, 449, pp. 336-347, 2016.

[25] Z. Zhou, Z. Han, Z.R. Lu. ''A targeted nanoglobular contrast agent from host-guest self-assembly for MR cancer molecular imaging'', *Biomaterials*, 85, pp. 168-179, 2016.

[26] Z. Miao, Y. Wang, R. Fierro. ''Collision-free consensus in multi-agent networks: A monotone systems perspective'', *Automatica*, 64, pp. 217-225, 2016.

[27] W. Ding, C. Lou, J. Qiu, Z. Zhao, Q. Zhou, M. Liang, Z. Ji, S. Yang, D. Xing. ''Targeted Fe-filled carbon nanotube as a multifunctional contrast agent for thermoacoustic and magnetic resonance imaging of tumor in living mice'', *Nanomedicine: Nanotechnology, Biology, and Medicine*, 12, pp. 235-244, 2016

[28] J. Ferber. *Multi-Agent System: An Introduction to Distributed Artificial Intelligence*. Addison Wesley Longman, Harlow 1999.

[29] A.M. Florea. *Introduction to Multi-Agent Systems*. International Summer School on Multi-Agent Systems, Bucharest, 1998.

[30] J. Liu, Y.Y. Tang. ''Adaptative image segmentation with distributed behavior based agents'', *IEEE Trans. Pattern Anal. Mach. Intell.* 6, pp. 544-551, 1999.

[31] V. Rodin, F. Harrouet, P. Ballet, J. Tisseau. ''oRis: Multiagents Approach For Image Processing'', in: *H. Shi, P.C. CoJeld (Eds.), SPIE Conference on Parallel and Distributed Methods for Image Processing II, 3452, SPIE, San Diego, CA*, pp. 57-68, 1998.

[32] E.G.P. Bovenkamp, J. Dijkstra, J.G. Bosch, J.H.C. Reiber. ''Multi-agent segmentation of IVUS images'', *Pattern Recognition*, 37, pp. 647-663, 2004.

[33] H. Settache, C. Porquet, S. Ruan. *Une plate-forme multi agents pour lasegmentation d'images: application dans le domaine des IRM cérébrales 2D*, Technical report, Université de Caen, 2002.

[34] F. Bellet. *Une approche incrémentale, coopérative et adaptative pour la segmentation des images en niveau de gris*. Institut National Polytechnique de Grenoble, France, 1998.

[35] K. Yanai. *An image understanding system for various images based on multi-agent architecture*, 1999.

[36] K. E. Melkemi, M. Batouche, S. Foufou. ''A multiagent system approach for image segmentation using genetic algorithms and extremal optimization heuristics'', *Pattern Recognition Letters*, 27, pp. 1230-1238, 2006.

[37] A. Kasaiezadeh, A. Khajepour, S.L. Waslander. ''Spiral bacterial foraging optimization method'', in: *American Control Conference, ACC2010, Baltimore, Maryland, USA*, 2010.

[38] D. Levine. *User's guide to the PGAPack parallel genetic algorithm library*, T.R.ANL-95/18, Algonne National Laboratory, 1996.

[39] FIPA: Foundation for Intelligent Physical Agents, « Agent Communication Language », FIPA 99 Specification Draft, 1999.

[40] S. Caraiman, V. I. Manta. ''Histogram-based segmentation of quantum images'', *Theoretical Computer Science*, pp. 46-60, 2014.

[41] M. A. Gungor, I. Karagoz. ''The homogeneity map method for speckle reduction in diagnostic ultrasound images'', *Measurement*, 68, pp.100-110, 2015.

[42] *Agent Communication Language*, FIPA Foundation for Intelligent Physical Agents, Specification Draft, 1999.

[43] Matlab, Help, "sections: Visualizing MRI data: Volume Visualization Techniques (3-D Visualization) ", Image Processing Toolbox.

[44] J. L. Liu, D. Z. Feng. ''Two-dimensional multi-pixel anisotropic Gaussian filter for edge-line segment (ELS) detection'', *Image and Vision Computing*, 32, pp. 37-53, 2014.

[45] D. Demigny. ''On optimal linear filtering for edge detection'', *IEEE Trans. Image Process*, 11 (7), pp. 728-1120, 2002.

[46] Y. Jinhua, Y. Wang, Y. Shen. ''Noise reduction and edge detection via kernel anisotropic diffusion'', *Pattern Recogn. Lett*. 29, pp. 1496-1503, 2008.

[47] A. Nachour, L. Ouzizi, Y. Aoura. ''Femur 3D Reconstruction from MR images'', *International Journal of mathematics and computation*, pp. 43-51, 2015.

[48] M. Kass, A. Witkin, D. Terzopoulos. ''Snakes: active contour models'', *Computer Vision* (1), pp. 21-31, 1988.

[49] P. Gamage, S.Q. Xie, P. Delmas, W.L. Xu. ''Diagnostic radiograph based 3D bone reconstruction framework: Application to the femur''. *Computerized Medical Imaging and Graphics*, 35, pp. 427- 437, 2011.

Authors Biographies

abdelhafid NACHOUR He received his Bachelor of experimental science in 2006, and Master of Informatics and computer vision degrees from Faculty of science fez, Morocco in 2013. His research interests include imageprocessing and 3D reconstruction.

Youssef AOURA is an associate professor at the National Higher School of Engineering (ENSAM Meknès - Moulay Ismail University, Morocco). He obtained his Ph.D. thesis in Manufacturing Processes from the

National Higher School of Engineering (ENSAM – France, in 2004). His research work is dealing with optimisation of new products and manufacturing processes.

Latifa OUZIZI is an associate professor at the National Higher School of Engineering (ENSAM Meknès - Moulay Ismail University, Morocco). He obtained his Ph.D. thesis in Automatic and Productic from Metz; University Metz France, in 2005. His research work is dealing with imaging, optimisation of new products, PLM and supply chain management.